

K I emission from envelopes around N-type stars – Spectroscopic observations and interpretations

Bengt Gustafsson¹, Kjell Eriksson¹, Dan Kiselman², Nils Olander³, and Hans Olofsson⁴

¹ Uppsala Astronomical Observatory, Box 515, S-751 20 Uppsala, Sweden

² The Royal Swedish Academy of Sciences, Stockholm Observatory, S-133 36 Saltsjöbaden, Sweden

³ Dept. of Physics and Mathematics, Mid Sweden University, S-851 70 Sundsvall, Sweden

⁴ Stockholm Observatory, S-133 36 Saltsjöbaden, Sweden

Received 15 April 1996 / Accepted 10 July 1996

Abstract. Circumstellar envelopes around three bright N-type stars, R Scl, X TrA, and V Aql have been detected in emission in resonance lines from K I. This radiation, which is most probably scattered photospheric radiation, was first found spectroscopically, but has later been imaged with coronagraphic and polarimetric techniques. In the present paper, which is the first in a series, the spectroscopic K I observations are discussed.

From the observations of the K I 769.9 nm emission we find systemic and expansion velocities in fair agreement with those obtained from the CO millimetre lines. We find a decline of the emission with distance from the star, in rough agreement with the assumption of a constant expansion velocity, mass-loss rate and K I abundance. Our mass loss rate estimates from the K I line observations agree rather well with those obtained from CO (ranging from 1/4 to 1/1 of the CO mass loss), which suggests that a considerable fraction of the potassium stays neutral through the envelope. This puts strong upper limits on the photoionizing chromospheric UV emission from the stars. Some indirect indications that the envelopes have inhomogeneous structures, clumps, are discussed.

Key words: stars: carbon – circumstellar matter – stars: individual: R Scl, X TrA, V Aql – stars: mass-loss – stars: AGB

1. Introduction

In a study of the chromospheric Mg II h & k emission of the bright N-type carbon star TX Piscium with the IUE we found that the Mg II lines were severely blended by resonance lines of Mn I and Fe I in absorption (Eriksson et al. 1986). Simple estimates of the column densities needed to produce this absorption made us search for a circumstellar envelope around the star at CO mm wavelengths. This search led to a positive identification, and later we found that the vast majority of the apparently

brightest N-type stars in the near infrared show circumstellar CO emission (Olofsson et al. 1988, 1993). We also found that about 5% of these CO line profiles show signatures that indicate envelopes that are markedly detached from the stellar surface, and we later verified this interpretation by detailed maps of four stars, which showed that the CO line emitting gas was distributed in the form of large, and geometrically thin, shells centred on the stars (Olofsson et al. 1992, 1996). One interpretation of this fact that agreed with physical and statistical data was that the detached shells are produced in connection with helium burning that occurs in short pulses, flashes, on the later part of the evolution along the asymptotic giant branch (cf. Olofsson et al. 1990). The maps of the sources with detached shells indicated that the shells are almost entirely empty, at least of CO, so that the mass loss was suggested to be switched off, after a probable rapid increase, as a result of the shell flash. We also found, from the detailed maps, that the CO emission indicated a clumpy circumstellar medium, with each shell consisting of apparently several tens of CO clumps (Olofsson et al. 1992, 1996; Bergman et al. 1993). Since the poor spatial resolution of single radio telescopes limits the map resolution to typically 10'' we decided to search for the shells also at visual and near infrared wavelengths, i.e. as scattered photospheric emission in the Na D and K I 769.9 nm resonance lines. If detections could be made, these data could be expected to be complementary to the CO data since they sample the interior parts of the shell, in view of the decline of the illuminating radiative flux with the distance from the stellar surface.

The envelopes around several red giants (α Ori, Bernat & Lambert, 1975, 1976, Bernat et al. 1978, Honeycutt et al. 1980, Maun & Caux 1992, and references therein; μ Cep, Maun et al. 1986, Maun & Querci 1990; R Leo, Lambert & van den Bout 1978; α^1 Her and o Cet, Maun & Caux 1992, g Her and the miras R Aql, R Leo and V Hya, Plez & Lambert 1994; ρ Per, β Peg and CE Tau, Maun & Guilain 1995, and the miras W Hya and R Hya, Guilain & Maun 1996) have been traced and studied in these lines; for some stars in considerable detail with important scientific results. V Hya is the only carbon star

Send offprint requests to: B. Gustafsson

envelope that has been investigated with this method, except the carbon-rich planetary nebula BD+30°3639, from which Dinerstein & Sneden 1988 reported Na I emission. Guilain & Maun (1996) report lower limits on the K I emission from the carbon stars TX Psc, Y CVn and U Hya.

We made the first discovery for R Scl (reported in Edvardsson 1990) with the CAT-CES at ESO, both in the Na D and the K I 769.9 nm line. These studies continued for this star and for others with the same equipment at several subsequent observing runs. With the Nordic Optical Telescope, and with the ESO 2.2 m, we also tried direct imaging with coronagraphic methods, starting in 1991, however, with little success. The problems clearly are due to the faintness of the envelope which makes the scattered light from the star in the atmosphere or the telescope very problematic. However, in 1994 we succeeded to image the envelopes of several stars with the ESO 3.6 m telescope.

Subsequently we present the spectroscopic observations of the K I line in Sect. 2, and discuss the results in Sect. 3. The results of the Na I and imaging observations are discussed in later papers.

2. Observations, reductions and results

The spectroscopic observations were carried out at four different runs, in February and September 1989, in August 1990, and in August 1994, at the ESO 1.4 m CAT and the CES spectrometer. The slit width was set to 0.47 mm, corresponding to $1.7''$ on the sky. The spectral resolution was 53,000. A number of different slit positions were tried, with the star in the slit, with the star outside the slit in the slit direction, with the star on either side of the slit in the cross direction at different distances, from a few seconds of arc to more than $20''$. Exposure times ranged from a few minutes at on-star positions, to 3 hours. Typical observing times for the off-star positions were $1\frac{1}{2}$ hours. One should note that with the alt-alt mounting of the CAT this means that the spectrometer slit changes its position angle about 30 degrees during the exposure, so that the observed envelope spectrum is a mean of a fairly extended section of the envelope.

17 bright carbon stars with CO detections were chosen as targets – spectroscopic evidence of envelope emission was found for three of them, R Scl, V Aql and X TrA, and only observations of these are discussed subsequently. (It should be remarked that the first positive discovery of envelope emission for R Scl was made in remote observing mode, with the observer operating from Garching near Munich.) For calibration purposes we also observed some early-type stars. The observed spectrum frames were, after subtraction of bias, divided by a lamp flat field. Next, the spectra were wavelength calibrated by means of Th lamp spectra. After that, the off-star spectra were subtracted by the on-star spectrum, scaled to the same overall “continuum level”, in an attempt to subtract the stellar component that is scattered into the envelope spectrum by the Earth’s atmosphere and the telescope/spectrometer. This was made individually for each pixel row on the detector perpendicular to the slit direction.

The results of this procedure are illustrated in Fig. 1 and 2. It is obvious from Fig. 1 that already in the raw off-star spectrum

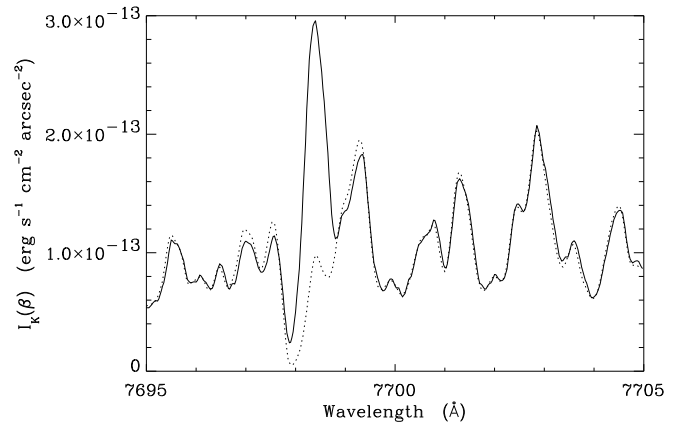


Fig. 1. An off-star spectrum ($\beta \approx 6''$) for R Scl at the K I line position. The dotted line is an on-star spectrum, which was scaled by about a factor of 0.0016.

of R Scl with no subtraction made one may trace an emission component, although the complex line spectrum does not admit any safe conclusions on the strength of the emission component until the subtraction is made. In Fig. 2 the subtracted spectra of the envelope of R Scl are displayed for different distances from the star.

The calibration of the spectra in absolute fluxes (on Earth) was made by means of the observations of early-type stars. The fluxes were estimated from the observed count rates, the differences in apparent magnitudes, in exposure times and zenith distances between the programme stars and the calibration stars, the colour differences and using the absolute calibration for Vega by Hayes & Latham (1975). This only results in rough fluxes; they may be in error by about a factor of 3. However, considering the other uncertainties in the estimates to follow, this is satisfactory. Also, the relative fluxes at different locations in the envelope are far more accurate. Moreover, for the mass-loss estimates to be described below, we are only dependent on the measured emission-line fluxes relative to the stellar fluxes at the corresponding wavelengths; quantities which are not dependent on the absolute calibration.

In Fig. 2 we display spectra from two different slit positions on the envelope around R Scl and it is seen that the line profiles are significantly different in the two different slit orientations, albeit fluxes come from regions at roughly the same distance from the star. In Fig. 3 spectra of the envelope of X TrA are shown, in Fig. 4 those for V Aql, and in Fig. 5 the sodium D-lines of R Scl are shown without subtraction of the photospheric spectrum. Clearly, the envelope emission is also visible in these lines. Fig. 6, finally, displays the K I line region for a star, S Sct, where no emission could be detected spectroscopically.

Our observations of the Na D line regions are less complete, less homogeneous and more affected by blends than the K I 769.9 nm observations. Therefore, in the present discussion we concentrate on the K I data.

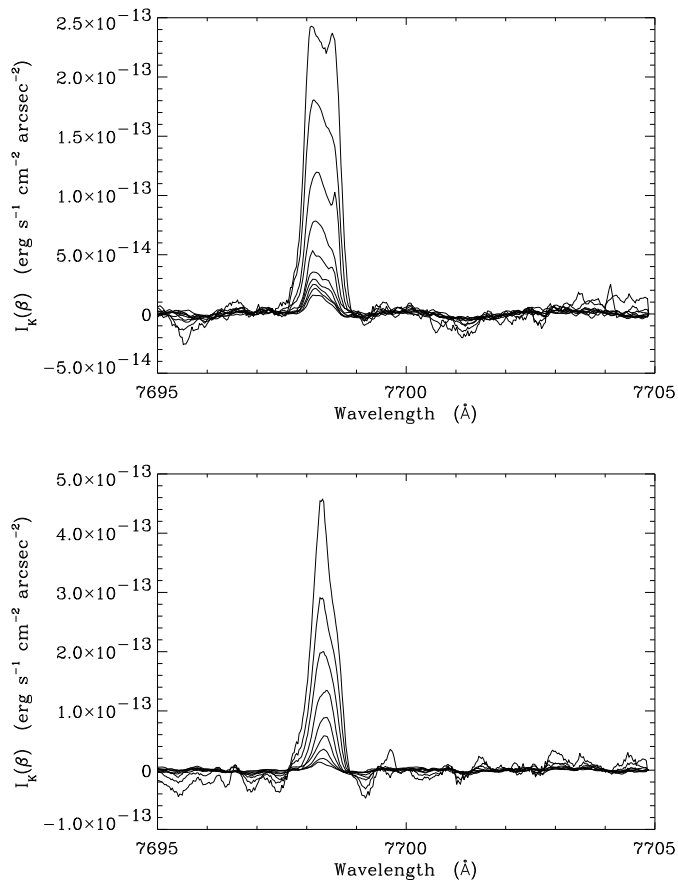


Fig. 2. The subtracted K I spectra (off-star minus scaled on-star) for different distances from R Scl. In this case the star was located outside the slit in its direction, about $4''$ away from the slit end. The top spectrum represents the emission about $4''$ from the star, the following at a distance of $0.83''$ further away, the next spectrum with another increment of $0.83''$ in the distance, etc. The two figures are for two different position angles.

3. Analysis

3.1. Wavelengths

The wavelengths of the envelope emission, as observed in the subtracted spectra, have been measured and agree nicely with the observed CO emission velocity. The systemic velocities relative to the local standard of rest, $V(\text{K I})$, as estimated from the centre of gravity of the K I emission, and the expansion velocities, $v_e(\text{K I})$, as judged from the width of the emission corrected for the finite resolution of the spectrograph, are presented in Table 1. For comparison the corresponding quantities from the CO observations by Olofsson et al. (1993) are also given. The overall agreement with the measured CO velocities is gratifying.

Another interesting fact is that for two of the stars, V Aql and X TrA, the wavelength of the deep centre of the absorption line in the on-star spectra agrees with the wavelength of the top of the emission feature in the subtracted spectra minus the half-width of the emission line. This suggests that the absorption is formed in the circumstellar gas expanding in the line of the

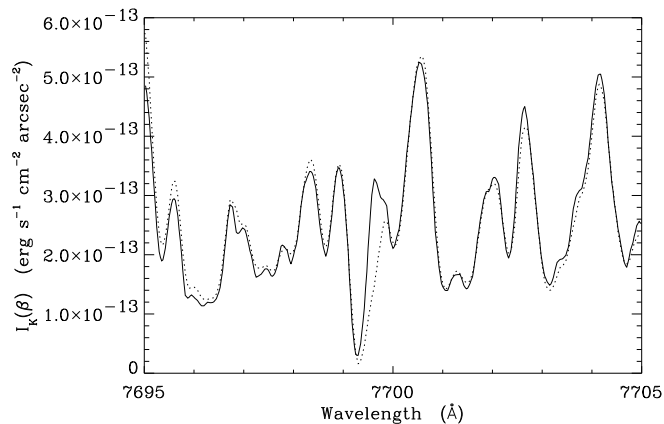


Fig. 3. K I spectrum of the envelope around X TrA at a distance from the star of $4''$. The dotted line denotes a scaled on-star spectrum.

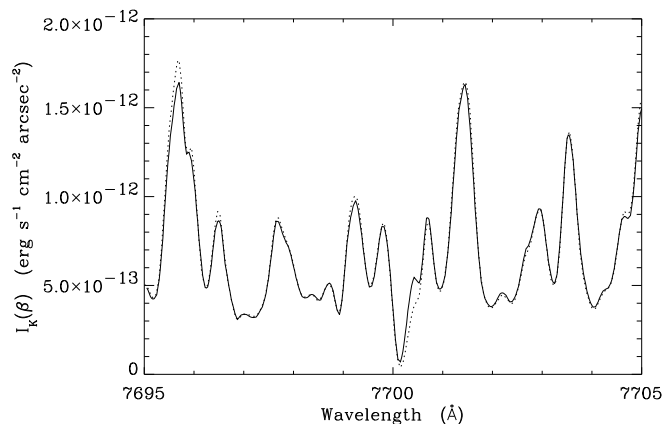


Fig. 4. K I spectrum of the envelope around V Aql at a distance from the star of $3''$. The dotted line denotes a scaled on-star spectrum.

sight from the star. (Some interference – however, not of great significance for conclusions given in this paper – may also be due to interstellar absorption. E.g., for V Aql, located close to the plane of the Galaxy, interstellar components can be easily traced in the sodium D lines.) For R Scl the centre of the absorption line is shifted a few km/s to the red, suggesting a somewhat smaller expansion velocity in this direction or, possibly, interference from interstellar absorption for this star which is at the largest distance of the programme stars. It is also possible that the CO envelope of this star, which is resolved in the CO(3-2) line observations as a “detached shell source” (Olofsson et al. 1996) is physically distinct from and expands more rapidly than the K I line forming region. Also, note that Olofsson et al. (1996) find a smaller velocity (of $\approx 10 \text{ km s}^{-1}$) for the inner regions of the CO envelope.

3.2. Line intensities and mass-loss rates

We have integrated the K I profiles of the three stars for all the subtracted spectra and thus deduced the flux in the emission

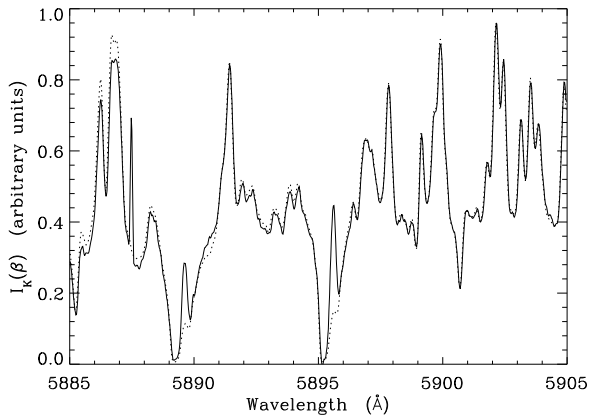


Fig. 5. Na I spectra of R Scl. Solid line is the off-star spectrum at a distance from the star of 5'', and the dotted line the scaled on-star spectrum.

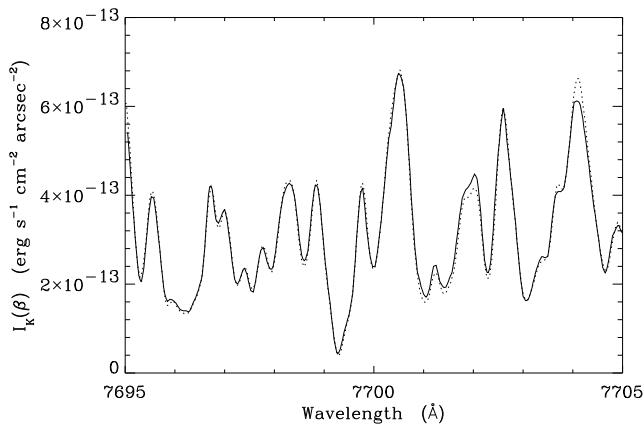


Fig. 6. K I spectrum of the envelope around S Sct at a distance from the star of 4''. The dotted line denotes a scaled on-star spectrum.

line as a function of angular distance from the star. The strength of the emission as a function of position angle is different in different directions, an effect which is seen in Fig. 7. However, for the programme stars we have not found any asymmetries as strong as the bipolar jet around V Hya (cf. Plez & Lambert 1994). The dependence of the emission on position angle has not been investigated systematically yet, and one should therefore not take the results displayed in Fig. 7 as more than indicative. A rapid decrease of the emission with the distance from the star seems, however, to be characteristic for all the three envelopes observed. A typical upper limit of the envelope emission from the 14 stars where no detection was made is 10^{-14} ergs s^{-1} cm^{-2} arcseconds $^{-2}$.

We shall now construct a simple spherically symmetric model for the envelope, assumed to be optically thin. Somewhat similar models have been constructed earlier, see, e.g. Bernat (1976), Mauron & Caux (1992) – we give however the expressions needed below for further use. It should be stressed, that a more satisfying treatment of the radiative transfer in spherically

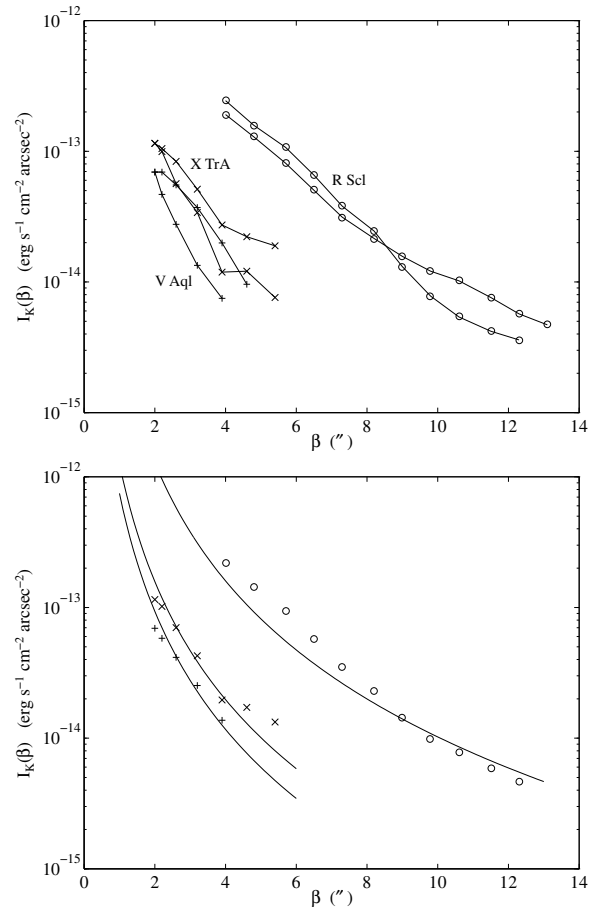


Fig. 7. The wavelength-integrated circumstellar K I emission $I_K(\beta)$ as a function of the angular distance β to the stars. Top panel: the observed values at different slit orientations for the three stars. Bottom panel: β^{-3} fits are shown together with the mean of the observed values.

symmetric expanding envelopes is needed for more detailed and definitive conclusions. This will be the subject of a forthcoming study. One may easily derive the following expression for the ratio between the wavelength integrated flux $f(p)$ received in a scattered line on Earth from a column with a cross-section area δA in the envelope at a minimum distance (“impact parameter”) p from the star, relative to the observed stellar flux \bar{f}_λ (averaged across the line width in the laboratory frame, $\delta\lambda$):

$$\frac{f(p)}{\bar{f}_\lambda} = \frac{\sigma_\lambda \delta\lambda \delta A}{4\pi} \int_{-\infty}^{\infty} \frac{N_{\text{scat}}(r)}{r^2} dz. \quad (1)$$

Here, σ_λ is the cross section of the scattering process and $N_{\text{scat}}(r)$ is the number of scattering particles per cm^3 at a distance $r = \sqrt{z^2 + p^2}$ from the star. For a constant mass loss rate \dot{M} , with a constant velocity v_e one finds

$$N_{\text{scat}}(r) = \frac{\dot{M}}{4\pi r^2 v_e} n_{\text{scat}}, \quad (2)$$

where n_{scat} is the number of scatterers per gram matter. Assuming n_{scat} to be independent of r , performing the integral and

measuring $I_K(\beta)$ – the wavelength integrated intensity in the scattered line in units of $\text{erg s}^{-1} \text{cm}^{-2} \text{arcseconds}^{-2}$ – with β being the distance in seconds of arc from the star, one finds

$$\dot{M} = \frac{32\pi}{206265} \frac{d v_e}{\sigma_\lambda \delta\lambda n_{\text{scat}}} \frac{I_K(\beta)}{\bar{f}_\lambda} \beta^3. \quad (3)$$

Here, d is the distance to the star from the Earth. For atomic scattering, one finds

$$\sigma_\lambda = \frac{\pi e^2 \lambda^2 f}{m_e c^2 \delta\lambda} \quad (4)$$

and $n_{\text{scat}} = \epsilon_{\text{KI}}/(\mu m_{\text{H}})$, leading to

$$\frac{I_K(\beta)}{\bar{f}_\lambda} = \frac{206265}{32} \frac{e^2 \lambda^2}{m_e c^2 m_{\text{H}}} f \dot{M} \frac{\epsilon_{\text{KI}}}{\mu v_e d} \left(\frac{1}{\beta}\right)^3. \quad (5)$$

Here, ϵ_{KI} is the abundance of neutral potassium relative to hydrogen, assumed to stay constant through the envelope. e and m_e are the electron charge and mass, respectively, m_{H} the hydrogen atomic mass, λ the wavelength, f the oscillator strength of the line, μ the mass density of matter relative to the density of hydrogen. As a test of this relation we have plotted the measured flux ratios in Fig. 7 for the three envelopes as a function of the angular distance to the central star. In this figure the means of the fluxes in two different slit directions are plotted. Fig. 7 suggests that there are differences in intensity between different slit directions on the sky, but in view of the uncertainties in the measurements and calibrations we still consider these indications tentative. Obviously the β^{-3} dependence gives a reasonably good description of the observations, although there are indications that the intensity increase falls below this relation in the inner shell region. Eq. (3) offers a possibility to make independent estimates of the mass loss rates. Adopting a value of ϵ_{KI} of $1.35 \cdot 10^{-7}$, which is the solar abundance of potassium (Anders & Grevesse, 1989 – which is not inconsistent with the meagre knowledge available on metal abundances for these stars, cf. Lambert et al. 1986 – we tentatively assume all potassium to be in neutral atomic form) and with relevant numbers one obtains

$$\dot{M} = 2.2 \cdot 10^{-10} v_e d \beta^3 \frac{I_K(\beta)}{\bar{f}_\lambda} \quad (\text{M}_\odot \text{yr}^{-1}), \quad (6)$$

where v_e is given in km s^{-1} , d in parsec, β in seconds of arc, $I_K(\beta)$ in $\text{ergs s}^{-1} \text{cm}^{-2} \text{arcseconds}^{-2}$ and \bar{f}_λ in $\text{ergs s}^{-1} \text{cm}^{-2} \text{\AA}^{-1}$.

In using Eq. (6) for estimating mass-loss rates we have determined $I_K(\beta)/\bar{f}_\lambda$ relatively far out in the K I envelope, at β values given in Table 1. We have taken velocities from the CO observations (Olofsson et al. 1993, OEGC); however they are compatible with the optical observations, see above, and those could have been adopted as alternatives. The stellar distances were also taken from Olofsson et al. and the resulting mass loss rates are compared with their mass loss rates, estimated from CO emission, in Table 1.

A reasonably good agreement is obtained between the resulting mass loss rates and those based on CO observations,

Table 1. Data for the three stars with detected K I envelopes

	R Scl	V Aql	X TrA
$V(\text{K I})$ (km s^{-1})	-18	54	0
$V(\text{CO})$ (km s^{-1})	-19.1	54.2	-2.0
$v_e(\text{K I})$ (km s^{-1})	15	9	8
$v_e(\text{CO})$ (km s^{-1})	16	7.6	7.8
d (pc)	420	390	320
β (")	10	4	5
$I_K(\beta)/\bar{f}_\lambda$	$3.2 \cdot 10^{-4}$	$6.3 \cdot 10^{-4}$	$1.1 \cdot 10^{-3}$
$p_{\tau=1}$ (cm)	$4 \cdot 10^{16}$	$9 \cdot 10^{15}$	$3 \cdot 10^{16}$
$\beta_{\tau=1}$ (")	6.2	1.7	5.5
$\dot{M}(\text{Eq. (6)})(\text{M}_\odot \text{yr}^{-1})$	$5 \cdot 10^{-7}$	$3 \cdot 10^{-8}$	$8 \cdot 10^{-8}$
$\dot{M}(\text{OEGC})(\text{M}_\odot \text{yr}^{-1})$	$1.7 \cdot 10^{-6}$	$9.4 \cdot 10^{-8}$	$1.0 \cdot 10^{-7}$
$\dot{M}(\text{Eq. (11)})(\text{M}_\odot \text{yr}^{-1})$	$6 \cdot 10^{-6}$	$3 \cdot 10^{-7}$	$2 \cdot 10^{-6}$

suggesting that the basic assumptions behind our model are essentially correct. We note in particular that severe ionization of potassium, a lower mass loss rate after the ejection of the (outer) CO envelope or an optically thick envelope in the K I lines should show up as systematically lower mass-loss estimates from the optical observations.

3.3. Are the envelopes optically thin?

As a more direct test of the assumption of the optical thinness of the envelope we estimate the optical depth of a column of the envelope at a minimum distance p from the centre. We find

$$\tau \approx \int_{-L/2}^{L/2} \frac{e^2 \lambda^2}{m_e c^2 m_{\text{H}}} \frac{f}{\delta\lambda} \dot{M} \frac{\epsilon_{\text{KI}}}{\mu v_e} \frac{1}{4p^2} dl, \quad (7)$$

where the integral is to be extended across a part of the envelope where the differential Doppler shift is small enough as compared with the line width, i.e.

$$L \approx p \frac{\delta\lambda}{\lambda} \frac{c}{v_e}. \quad (8)$$

Eqs. (7) and (8) then give for the ‘‘impact parameter’’ p at which $\tau \approx 1$,

$$p_{\tau=1} \approx 2.0 \cdot 10^{25} \frac{\dot{M}}{v_e^2} \quad (\text{cm}), \quad (9)$$

with \dot{M} in $\text{M}_\odot \text{yr}^{-1}$ and v_e in km s^{-1} . One should note that the line profile width, $\delta\lambda$, does not enter here, since the range of the integral diminishes in proportion to the increase in the peak value of the line profile with decreasing $\delta\lambda$.

The impact parameters $p_{\tau=1}$ and the corresponding angular distances $\beta_{\tau=1}$, where the optical depths along a column through the envelopes become 1, are listed in Table 1. Obviously, the assumption that the envelope is optically thin in the regions where the fluxes are measured for the mass estimate is verified, i.e., $\beta_{\tau=1}$ is indeed smaller than β for two stars, R Scl and V Aql. For X TrA the case is marginal in the sense that $\beta_{\tau=1} \approx \beta$. It should be noted that this does not mean that the envelopes are

optically thin radially into an angular distance of β ; instead the radial depths are one order of magnitude greater than 1, as a result of the lack of a velocity gradient along the radii. However, this does not invalidate our mass loss estimate according to Eq. (6) as long as \bar{f}_λ , which we estimate from the measured on-star spectrum, can be taken to be representative for the stellar spectrum that reaches the envelope gas at a point at angular distance around β .

3.4. Are the envelopes ionized?

We shall now address the question what ionization conditions are to be expected in the envelopes. The model calculations of Glassgold & Huggins (1986) for the circumstellar envelope of α Ori suggest fractions of neutral K I relative to K I+K II of the order of 1% in the envelope. This reflects the high photoionization rate due to chromospheric UV radiation from the star. In particular radiation in the wavelength interval from 170 nm to 250 nm is of significance. At longer wavelengths – approaching the ionization threshold at 285.5 nm – the photoionization cross section gets very small due to overlapping wave functions. The knowledge about the ultraviolet fluxes from the chromospheres of N-type stars is very restricted; the best studied case being TX Psc (Eriksson et al. 1984, Johnson et al. 1996) but also for this star nothing is known about the flux shortwards of 230 nm. Also, the circumstellar absorption of that flux may be expected to be severe; we note that the IUE spectrum of the hot central star in the Red Rectangle object suggests that a carbon-rich envelope may produce a very strong absorption shortwards of 145 nm (Sitko et al. 1981, Mauron & Caux 1992). Extrapolating the TX Psc flux to shorter wavelengths Mauron & Caux (1992) estimate that, at a distance of 4'' for that star (corresponding to $1.7 \cdot 10^{16}$ cm) the stellar photoionization rate is of the same order of magnitude as the interstellar one which they estimate to be $G_{\text{int}} \approx 4.6 \cdot 10^{-11} \text{ s}^{-1}$. This interstellar flux is great enough to significantly reduce the K I density in our observed envelopes within their timescales. Since the stellar photoionization rate scales as r^{-2} , where r is the distance from the star, one would obtain as a rough estimate for the photoionization rate G_\star due to the UV flux from a TX Psc-like chromosphere:

$$G_\star(r) = 1.3 \cdot 10^{22} r^{-2} \quad (\text{s}^{-1}, r \text{ in cm}). \quad (10)$$

In order to explore the role of the recombinations, we have complicated our model by adopting the basics of the model developed for the envelope of TX Psc of Mauron & Caux (1992), with their extrapolated chromospheric TX Psc flux, the electron density x_e relative to hydrogen set to $2 \cdot 10^{-5}$, and a characteristic envelope temperature of 30K, with a smooth temperature variation with radius (the precise form of which, however, is not very significant). The envelope emission is proportional to a quantity I_r (see Mauron & Caux 1992, Eqs. (2) and (A1)) which is somewhat dependent on the temperature distribution but in particular on the ratio of stellar to interstellar K I photoioniza-

tion rates. From Eq. (2) of Mauron & Caux (1992) we derive, with the same symbols and units as in Eq. (6) above,

$$\dot{M} = 2.1 \cdot 10^{-8} v_e d^{1/2} \beta^{3/2} I_r^{-1/2} \left(\frac{I_K(\beta)}{\bar{f}_\lambda} \right)^{1/2}. \quad (11)$$

(The difference between this relation and Eq. (6) as regards the different dependence on $d \cdot \beta^3 \cdot I_K(\beta)/\bar{f}_\lambda$ originates in the density dependence of the recombination rate.) Following Mauron and Caux in their choice of $I_r=0.4$ for TX Psc, we derive the mass loss rates listed in the last row of Table 1. It is obvious that these mass loss rates are significantly higher than those derived from Eq. (6), basically reflecting the effects of ionization by a factor of about 10. This, however, does not explain the approximate β^{-3} dependence inside $\beta_{\tau=1}$ in Table 1 since the increased ionization would be compensated for by higher estimates of \dot{M} and envelope density, so that the transparency of the envelope would only increase marginally.

The mass loss rates derived from Eq. (11) are significantly larger than those derived from the CO observations. The latter may, however, be systematically underestimated as a result of, e.g., the neglect of the possible clumpiness of the shells (Olofsson et al. 1993, 1996; note that in the former paper the mass loss rate of R Scl is estimated to be $1.7 \cdot 10^{-6} M_\odot \text{ yr}^{-1}$ using a simple formula, while in the latter paper, where the clumpiness is taken into account and the radiative transfer is treated in some detail, the result is $8 \cdot 10^{-6} M_\odot \text{ yr}^{-1}$. For this star, however, it may well be that the scattered light comes from the inner envelope, while the CO emission originates in an outer shell, with higher expansion velocity, as the radial velocity difference may suggest). Conversely, a clumpy structure will increase the recombination rates and thus diminish \dot{M} (Eq. (11)) in proportion. Anyhow, it is not possible to discard the application of the Mauron & Caux (1992) model for these envelopes on the basis of the discrepancy in Table 1 between its last two rows. One should also note that the photoionisation cross-section of the K I ground state is less well known than one would desire. We have considered alternatives to the experimental data of Hudson & Carter (1965, 1967) that were used by Mauron & Caux (1992). The Hudson & Carter data is superseded by the experiments of Sandner et al. (1981) around the cross-section minimum at 270 nm but our calculations show that this has minimal impact on the rates. The computed values of Rahman-Attia et al. (1986) are significantly lower (by almost a factor of 2) than the Hudson and Carter cross sections in the most important wavelength region between 250 and 180 nm, but Rahman-Attia et al. consider the experimental data to be more reliable here.

Another conclusion from Table 1 is that the chromospheric UV fluxes from the programme stars should not be greater, and are probably smaller, than those adopted for TX Psc on the basis of extrapolations by Mauron & Caux (1992); see their Fig. 4. These, in turn, are one order of magnitude or more smaller than the fluxes observed for late type giants and supergiants. The discrepancy between real and assumed UV fluxes may well amount to a factor of 10 – the mass-loss rate scales as the square-root of the UV flux in Mauron & Caux Eq. (2), and a factor of

$\gtrsim 3$ in mass loss is needed to make the two last rows in Table 1 compatible.

One may wonder whether the fact that no K I emission could be traced from the majority of our 17 programme stars indicates that they have stronger chromospheric UV fluxes. That conclusion may, however, not be drawn; typical upper limits for their wavelength integrated K I envelope fluxes are only marginally below those observed for the three stars with clear detections. Moreover, smaller, or greater (see below), mass loss rates might also weaken the brightness of the envelopes.

3.5. Are the envelopes clumpy?

It is noteworthy that the envelope K I emission of R Scl varies roughly as β^{-3} further inside the estimated $\beta_{\tau=1}$ point, i.e. inside the point where the envelope is expected to be optically thick, which is contrary to the expected flattening of the profile. One interesting way of explaining the β^{-3} dependence inside $\beta_{\tau=1}$ in Table 1 would be to invoke a clumpy circumstellar gas – after all, clumps were traced in the CO observations of the more extended and detached shells (Olofsson et al. 1992, 1996, Bergman et al. 1993) and it would be of great interest if one could argue that the present observations indicate the existence of clumps in these smaller envelopes, much closer to the stars. If these clumps are of suitable size, with a radius δr , one might think that each of them could be optically thick at this relatively close distance to the central star, and act as an individual scatterer – we disregard from destruction of photons by collisional deexcitation – while the clumps could be rare enough to leave free paths for light in between them all the way out into empty space. This would preserve the β^{-3} dependence.

Another virtue of an inhomogeneous model is that because the recombination rate scales with the density it is considerably enhanced locally as compared with the homogeneous envelope model. Thus, the high mass loss estimates that result from efficient photoionization are moderated although the mass loss rate scales as the density in the clumps (cf. Eq. (13)).

It is easy to see that the condition for each clump to be optically thick is easily satisfied. The optical depth of a clump with density ρ is on the order of

$$\tau \approx \frac{\pi e^2 \lambda^2}{m_e c^2 m_H} \frac{f}{\delta \lambda} \frac{\epsilon_{\text{KI}}}{\mu} \rho \delta r. \quad (12)$$

We can now use Eq. (3) to derive a mass-loss rate for the clumpy medium, assuming all clumps to have the same radius and density. The cross section of each clump is $\pi \delta r^2$ and the number of clumps per mass unit is $n_{\text{scat}} = 1/(4/3 \pi \delta r^3 \rho)$, leading to

$$\dot{M} = \frac{128\pi}{3 \cdot 206265} \frac{I_{\text{K}}(\beta)}{f_{\lambda} \delta \lambda} d v_e \rho \delta r \beta^3. \quad (13)$$

From Eqs (5), (12) and (13) one finds the following condition for the individual clumps to be optically thick

$$\dot{M}(\text{Eq. (13)}) \gtrsim \dot{M}(\text{Eq. (6)}) \quad (14)$$

which is as expected.

The system should be optically thin, in the sense that the clouds do not overlap considerably along the line of sight, in order to preserve the β^{-3} dependence of the scattered emission. One clump has a mass along a column of 1 cm^2 cross section of typically $\rho \cdot \delta r$ grams. This mass should be larger than the mean mass in a column across the range L (cf. Eq. (8)) which is on the order of $\dot{M} \delta \lambda c / (4\pi p v_e^2 \lambda)$. Denoting the smallest angular distance from the star for which overlap does not occur by β_{lim} and expressing p in β_{lim} and d one then obtains

$$\rho \delta r \approx \frac{206265}{4\pi} \frac{\dot{M} c}{v_e^2 d \beta_{\text{lim}}} \frac{\delta \lambda}{\lambda}. \quad (15)$$

Eqs. (13) and (15) now lead to an expression which is independent of most parameters,

$$\beta_{\text{lim}} \approx \frac{32}{3} \frac{I_{\text{K}}(\beta)}{f_{\lambda} \lambda} \frac{c}{v_e} \beta^3. \quad (16)$$

With the fluxes of Table 1 this leads to values of β_{lim} ranging from $2''$ (V Aql) to $9''$ (R Scl). I.e., independently of most stellar parameters one can obtain the observed fluxes from a circumstellar medium arranged in clumps with so few clumps that they do not overlap on the sky for the outer parts of the observed envelopes. However, the β_{lim} values obtained makes it less probable that the problem with the β^{-3} dependence in the inner spherically symmetric envelope may be solved by adopting such a more inhomogeneous model.

Above, we have assumed all clumps to have the same radius which is certainly unrealistic. With an increasing clump size with radius (and time) which is physically most reasonable, one gets a slower decrease of the shell emission with radius. E.g., an expansion of the clump radius in proportion to the distance from the star would, for optically thick clumps, lead to a β^{-1} dependence, which is far from the observed slope. This may suggest that inhomogeneities are less pronounced in these inner regions than in the outer detached CO shells.

4. Conclusion

We have observed circumstellar K I and Na I emission from three N-type carbon stars and interpret this as resonance scattering of the photospheric light. We have found the dynamics of the envelopes, as seen in the potassium lines, to be reasonably consistent with what is deduced from the CO lines which sample regions further out in the envelopes. The intensities show a rough β^{-3} dependence which is expected for a constant mass loss rate, gas expansion velocity and K I abundance. An interesting and astonishing fact is that the intensities are large enough to suggest that a substantial fraction of the potassium in the envelope is in neutral form. This puts limits on the chromospheric UV emission (shortwards of the K I photoionization threshold at 285.5 nm) for these stars. Since mass loss is a regular phenomenon for N-type stars, with typical mass-loss rates of $10^{-7} M_{\odot} \text{ yr}^{-1}$ (Olofsson et al. 1993), an important aspect of

this is that the existence or non-existence of strong K I emission may be used as an indicator of the suppression or existence of chromospheric UV emission. Systematic deep surveys of K I emission for a sample of bright N-type stars, and observations of UV fluxes of those with the Hubble Space Telescope, would be rewarding to verify this connection which could then establish a new chromospheric indicator. Also time variations (in particular the “turning off”) of K I emission may be worth searching for. Another interesting fact is that the β^{-3} dependence of the envelope emission seems to continue inside the point in the envelope where the column optical depth should be > 1 . It seems possible, though not very probable, that this is due to inhomogeneities, clumps, in the envelope, similar in origin to those previously traced in detached CO shells. A more detailed modelling of radiative transfer and hydrodynamics in these media may be worthwhile, and seems necessary before more safe conclusions may be drawn.

One may ask why the objects which show K I emission in our survey all happen to have column optical depths around unity within the angularly resolved envelopes. This may well be a selection effect. Denser envelopes, corresponding to larger \dot{M} , should have smaller surface brightness, and so would considerably thinner envelopes. A deeper search to lower surface brightness for other N-type stars may be rewarding.

We finally note that the mass loss estimates from the K I emission scale as the distance d or $d^{1/2}$ to the star, while the CO mass loss estimate is proportional to d^2 . Thus, in principle distance estimates – indirect expansion parallaxes – are possible, though rather model dependent. Also, errors in adopted abundances may be significant and, in fact, comparisons of CO emission with K I or Na I emission might be used to estimate abundances of K and Na relative to O. However, improved models are needed before any of these possibilities may be exploited.

Acknowledgements. Olle Morell helped in carrying out some of the spectroscopic observations and Magnus Selhammar in the analysis of the results. Nils Ryde is thanked for checking the calculations and for giving valuable comments on the manuscript and Hugo Schwarz for valuable suggestions and active participation in following up this work with imaging observations. Harm Habing is also thanked for valuable comments on the manuscript. Financial support from the Swedish Natural Science Research Council is acknowledged.

References

- Anders, E., Grevesse, N., 1989, *Geochim & Cosmochim. Acta* 53, 197
 Bergman, P., Carlström, U., Olofsson, H., 1993, *A&A*, 268, 285
 Bernat, A.P., 1976, PhD thesis, Univ. of Texas
 Bernat, A.P., Lambert, D.L., 1975, *ApJ*, 201, L153
 Bernat, A.P., Lambert, D.L., 1976, *ApJ*, 210, 395
 Bernat, A.P., Bruhweiler, F.C., Kondo, Y., et al., 1978, *PASP* 90, 318
 Dinerstein, H.L., Sneden, C., 1988, *ApJ*, 335, L23
 Edvardsson, B., 1990, Uppsala Astronomical Observatory, *Ann. Rep.* 1989
 Eriksson, K., Gustafsson, B., Johnson, H.R., Querci, F., Querci, M., Baumert, J.H., Carlsson, M., Olofsson, H., 1986, *A&A*, 161, 305
 Glassgold, A.E., Huggins, P.J., 1986, *ApJ*, 306, 605
 Guilain, Ch., Maunon, N., 1996, *A&A*, 314, 585
 Hayes, D.S., Latham, D., 1975, *ApJ*, 197, 593
 Honeycutt, R.K., Kephart, J.E., Bernat, A.P. et al., 1980, *ApJ*, 239, 565
 Hudson R.D., Carter V.L., 1965, *Phys.Rev.*, 139, 1426
 Hudson R.D., Carter V.L., 1967, *J. Opt. Soc. Am.*, 57, 1471
 Johnson, H.R., et al., 1996, in preparation
 Lambert, D.L., van den Bout, P.A., 1978, *ApJ*, 221, 854
 Lambert, D.L., Gustafsson, B., Eriksson, K., Hinkle, K.H., 1986, *ApJS*, 62, 373
 Maunon, N., Cailloux, M., Tilloles, P., et al., 1986, *A&A*, 165, L9
 Maunon, N., Querci, F., 1990, *A&AS*, 86, 513
 Maunon, N., Caux, E., 1992, *A&A*, 265, 711
 Maunon, N., Guilain, Ch., 1995, *A&A*, 298, 869
 Olofsson, H., Eriksson, K., Gustafsson, B., 1988, *A&A*, 196, L1
 Olofsson, H., Carlström, U., Eriksson, K., Gustafsson, B., Willson, L.A., 1990, *A&A*, 230, L13
 Olofsson, H., Carlström, U., Eriksson, K., Gustafsson, B., 1992, *A&A*, 253, L17
 Olofsson, H., Eriksson, K., Gustafsson, B., Carlström, U., 1993, *ApJS*, 87, 267
 Olofsson, H., Bergman, P., Eriksson, K., Gustafsson, B. 1996, *A&A*, 311, 587
 Plez, B., Lambert, D.L., 1994, *ApJ*, 425, L101
 Rahman-Attia M., Jaouen M., Laplanche G., Rahman A., 1986, *J Phys B*, 19, 897
 Sandner W., Gallagher T.F., Safinya K.A., Guonand F., 1981, *Phys. Rev.*, 23, 2732
 Sitko, M.L., Savage, B.D., Meade, M.R., 1981, *ApJ*, 246, 161